

Steric Interference on the Redox-conjugated Pyrimidine Ring Rotation of Mono- and Dinuclear Copper Complexes with (4-Methyl-2-pyrimidinyl)imine Ligands

Yohei Hattori, Michihiro Nishikawa,[†] Tetsuro Kusamoto, Shoko Kume,^{††} and Hiroshi Nishihara*

Department of Chemistry, Graduate School of Science, The University of Tokyo, 7-3-1 Hongo, Bunkyo-ku, Tokyo 113-0033

(E-mail: nishihara@chem.s.u-tokyo.ac.jp)

A mononuclear copper(I) complex with *N*-[(4-methyl-2-pyrimidinyl)methylene]-*p*-toluidine (**1**·BF₄) and a dinuclear copper(I) complex with *N,N'*-bis[(4-methyl-2-pyrimidinyl)methylene]-*p*-phenylenediamine (**2**·(BF₄)₂) were synthesized as BF₄⁻ salts to evaluate the influence of the imine moiety on the pyrimidine ring rotation isomerism. **1**·BF₄ existed in solution as a mixture of two isomers; **2**·(BF₄)₂ was present as a mixture of three isomers. The redox potentials of the copper centers were changed by pyrimidine ring rotation. Comparison of **1**⁺ and **2**²⁺ indicated that increasing the steric congestion around the copper center increased the *o/i* isomer ratio; the redox potentials of both the *o*- and *i*-isomers shifted in the positive direction, and the Cu^{II/I} redox reaction became slower.

Molecular electronic devices and machines such as memories,¹ switches,² and motors³ have been developed as the components of ultimately accumulated computing system in the molecular scale. Molecular systems controlled by electrical stimuli are particularly expected to be important in future nanoelectronics.

Copper complexes are promising candidates for the molecular machinery system that is controlled by redox reactions (i.e., electrical stimuli) because of their reversible Cu^{II/I} redox activities, labile coordination bonds, and strong correlations between the coordination structure and Cu^{II/I} redox potential. Tetrahedral coordination is preferred by a Cu^I center, and square planar or five- and six-coordinated structures are preferred by a Cu^{II} center. Artificial molecular motors and muscles driven by the redox reactions of copper centers were reported by Sauvage et al.⁴

Our group previously reported the isomerizing motion of a copper complex [(L_{anth})Cu(L₃)]·BF₄ (**3**·BF₄, L_{anth}: 2,9-bis(9-anthryl)-1,10-phenanthroline, L₃: 4-methyl-2-(2'-pyridyl)pyrimidine).⁵ This complex exists in solution as a mixture of two isomers, an inner *i*-isomer and an outer *o*-isomer via 4-methylpyrimidine ring rotation, where *i*- and *o*- indicate the position of the methyl group on the pyrimidine ring. Although the structural difference between the isomers is solely the position of the methyl group, their Cu^{II/I} redox potentials differ by as much as 0.15 V. Therefore, on the basis of “coordination programming,”⁶ this molecule can behave as a molecular device that converts the rotational motion of the molecule into a redox potential. The copper complexes containing the 4-methyl-2-(2'-pyridyl)pyrimidine derivative ligands have been coupled with various auxiliary ligands, functional groups, or redox-active units to exhibit interesting properties; for example, electronic, magnetic, luminescent, mechanical, and light-driven properties.⁷

In this study, a mononuclear copper(I) complex [(L_{anth})Cu(L₁)]·BF₄ (**1**·BF₄ (Figure 1a), L₁: *N*-[(4-methyl-2-pyrimidinyl)methylene]-*p*-toluidine (Figure 1b)) was synthesized to

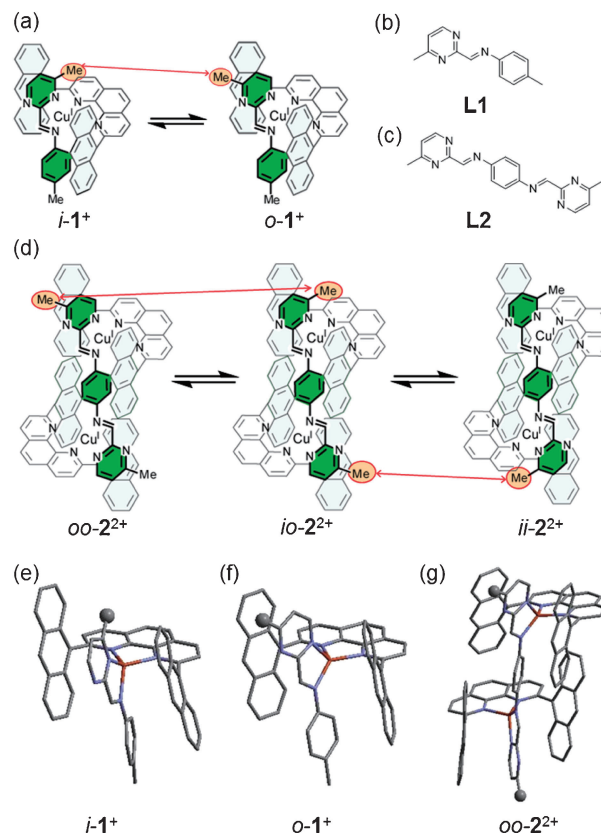


Figure 1. (a) *i*- and *o*-Isomers of **1**·BF₄. (b) *N*-[(4-Methyl-2-pyrimidinyl)methylene]-*p*-toluidine (**L1**). (c) *N,N'*-Bis[(4-methyl-2-pyrimidinyl)methylene]-*p*-phenylenediamine (**L2**). (d) *oo*-, *io*-, and *ii*-isomers of **2**·(BF₄)₂. (e) Molecular structure of *i*-**1**⁺ in [*i*-**1**]⁺·BF₄⁻·Et₂O crystal. (f) Molecular structure of one of *o*-**1**⁺ in [*o*-**1**]⁺·2BF₄⁻·3CH₂Cl₂·1.5*p*-xylene crystal. (g) Molecular structure of *oo*-**2**²⁺ in [*oo*-**2**]²⁺·(BF₄)₂⁻·*x*(solvents) crystal. Hydrogen atoms, BF₄⁻ anions and solvents are omitted for clarity. Methyl carbons on pyrimidine ring are shown as ball models.

evaluate the influence of the imine moiety on the pyrimidine ring rotation isomerism. We also prepared a dinuclear copper complex [(L_{anth})₂Cu₂(μ-L₂)](BF₄)₂ (**2**·(BF₄)₂ (Figure 1d), L₂: *N,N'*-bis[(4-methyl-2-pyrimidinyl)methylene]-*p*-phenylenediamine (Figure 1c)), in which two rotating 4-methylpyrimidine units are connected with a conjugated diimine skeleton. The aim of this study is to investigate the way in which the connection of the two units influences their rotational behavior and the redox characteristics of the copper centers. We report herein the synthesis, single-crystal X-ray crystallographic investigations, isomerization behavior, and redox properties of **1**·BF₄ and **2**·(BF₄)₂.

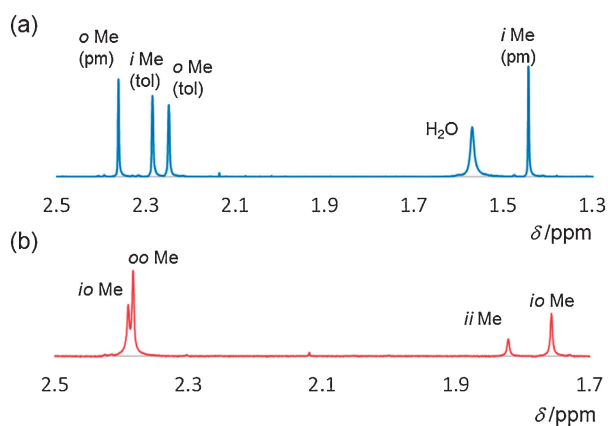


Figure 2. (a) ^1H NMR signals of methyl groups of $\mathbf{1}\cdot\text{BF}_4$ in CD_2Cl_2 (pm: methyl group on pyrimidyl group, tol: methyl group of tolyl group). (b) ^1H NMR signals of methyl groups of $\mathbf{2}\cdot(\text{BF}_4)_2$ in CD_2Cl_2 .

L1 and **L2** (Figures 1b and 1c) were each prepared from 4-methylpyrimidine-2-carbaldehyde with either *p*-toluidine or 1,4-phenylenediamine, respectively. $\mathbf{1}\cdot\text{BF}_4$ was synthesized by mixing a 1:1:1 molar ratio of $[\text{Cu}(\text{MeCN})_4]\text{BF}_4$, L_{anth} , and **L1** in CH_2Cl_2 at room temperature. $\mathbf{2}\cdot(\text{BF}_4)_2$ was yielded from a 2:2:1 mixture of $[\text{Cu}(\text{MeCN})_4]\text{BF}_4$, L_{anth} , and **L2**. The bulky 9-anthryl groups of L_{anth} impeded homoleptic complexation, resulting in the selective formation of heteroleptic complexes.¹⁰

Single-crystal X-ray diffraction studies revealed the structures of two linkage isomers of $\mathbf{1}\cdot\text{BF}_4$ (Figures 1e and 1f, Table S1).¹¹ The crystals obtained from a CH_2Cl_2 – Et_2O solution contained two crystallographically independent $\mathbf{1}\cdot\text{BF}_4$ ions, two BF_4^- ions, and two Et_2O molecules in the unit cell. The crystals from CH_2Cl_2 –*p*-xylene contained four $\mathbf{1}\cdot\text{BF}_4$ ions, four BF_4^- ions, three *p*-xylene molecules, and six Et_2O molecules. The labels *i*- and *o*- indicate the isomers of $\mathbf{1}^+$ with the methyl group in the inner and outer positions, respectively. These results indicate that the two isomers were similarly thermodynamically stable. This represents the first selective crystallization of both the isomers of the pyrimidine rotation system.

The ^1H NMR signals of $\mathbf{1}\cdot\text{BF}_4$ in CD_2Cl_2 were grouped into two sets, each attributable to one of the two isomers (*i* and *o*). The separation of the signals was supported by the ^1H – ^1H COSY spectrum (Figure S1). The signals were assigned on the basis of the shielding effect of the anthracene moieties,⁵ with a greater high-field shift of the methyl protons expected for the *i*-isomer ($\delta = 1.44$ ppm) than for the *o*-isomer ($\delta = 2.36$ ppm) (Figure 2a). Variable-temperature ^1H NMR spectra of $\mathbf{1}\cdot\text{BF}_4$ were measured from 203 to 303 K. The *o/i* ratio was calculated to obtain van't Hoff plots (Figure S2), which showed that ring inversion appeared to be frozen at below 263 K.

Cyclic voltammograms (CVs) of $\mathbf{1}\cdot\text{BF}_4$ recorded at 293 K show two redox waves at $E^{\circ'} = 0.56$ and 0.71 V vs. Ag^+/Ag (Figure 3a), indicating that $\mathbf{1}\cdot\text{BF}_4$ exists as a mixture of two isomers in the solution, corroborating the ^1H NMR results. The redox couple at more positive potential can be ascribed to the *i*-isomer and the other to the *o*-isomer. Because the methyl group of the *i*-isomer adjacent to the coordinating N atom prevents the formation of a favorable square-planar structure in the Cu^{II} state,¹² the *i*-isomer shows a more positive $E^{\circ'}$ value than did the *o*-isomer.

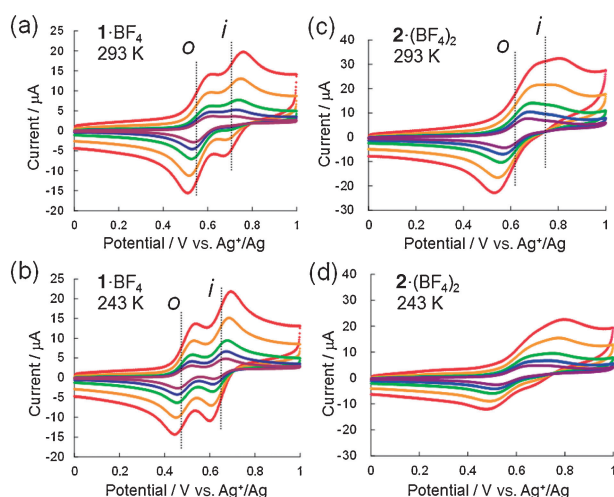


Figure 3. Cyclic voltammograms of $\mathbf{1}\cdot\text{BF}_4$ at 293 K (a), $\mathbf{1}\cdot\text{BF}_4$ at 243 K (b), $\mathbf{2}\cdot(\text{BF}_4)_2$ at 293 K (c), and $\mathbf{2}\cdot(\text{BF}_4)_2$ at 243 K (d) in dichloromethane with 0.1 M Bu_4NBF_4 as supporting electrolyte. Scan rates are 0.5 (red line), 0.25 (orange line), 0.1 (green line), 0.05 (blue line), and 0.025 V s^{-1} (purple line).

Decreasing the scan rate reduced the anodic peak current for the *i*-isomer more rapidly than for the *o*-isomer, indicating that the isomerization from the *i*-isomer to the *o*-isomer occurred over a time scale similar to the scan rate. The CVs of $\mathbf{1}\cdot\text{BF}_4$ recorded at 243 K show that the relative degree of peak current, indicating *o/i* was independent of the scan rate (Figure 3b). These results demonstrate that the ring inversion was blocked at this temperature, as evidenced by ^1H NMR.

Overall, $\mathbf{1}\cdot\text{BF}_4$ is shown here to work as a molecular device that converts rotational motion into a shift of redox potential in a way similar to that as previously reported for $\mathbf{3}\cdot\text{BF}_4$.⁵ Although they have similar functions, some differences in their properties emerge owing to structural factors.

XRD revealed distortion on the tetrahedral coordination environment of the copper center in $\mathbf{1}\cdot\text{BF}_4$. The angle α between the phenanthroline plane and the pyrimidine plane was investigated for the isomers as a measure of the degree of distortion: $\mathbf{1}\cdot\text{BF}_4$ each formed a distorted tetrahedral coordination environment with $\alpha = 77$ and 76° , respectively, while the pyrimidine plane was almost perpendicular to the phenanthroline plane ($\alpha = 87^\circ$) in a previously reported $\mathbf{3}\cdot\text{BF}_4$ crystal.⁵ The distortions are presumably due to the intramolecular π – π stacking interaction between the pyrimidinyl and anthryl groups. In the 2-(2'-pyridyl)-4-methylpyrimidine complex, such stacking would occur between the pyrimidinyl and anthryl groups and between the pyridyl and anthryl groups.

Structural effects also appear to influence the ratio of the isomers, with $\mathbf{1}\cdot\text{BF}_4$ showing a lower ratio (*i/o* = 1.1) than did $\mathbf{3}\cdot\text{BF}_4$ (*i/o* = 2.0) at 293 K owing to greater structural distortion of $\mathbf{1}\cdot\text{BF}_4$ causing greater steric congestion in the *i*-isomer. Electrochemical measurements revealed the $E^{\circ'}$ values of $\mathbf{1}\cdot\text{BF}_4$ (0.56 and 0.71 V vs. Ag^+/Ag) to be more positive than those of $\mathbf{3}\cdot\text{BF}_4$ (0.38 and 0.55 V vs. Ag^+/Ag).⁵ The difference was also attributed to steric effects; the tolyl group adjacent to the coordinating N atom prevents the formation of a favorable structure of Cu^{II} .

Single crystals of $2 \cdot (\text{BF}_4)_2$ obtained from a $\text{CH}_2\text{Cl}_2\text{-Et}_2\text{O}$ solution contained only the *oo*-isomer *oo*- 2^{2+} (Figure 1g, Table S2), which formed a symmetric molecular structure with an inversion center. The unit cell contains disordered solvent molecules in the void surrounded by *oo*- 2^{2+} and two BF_4^- ions.¹³

The coordination tetrahedron of 2^{2+} was more distorted ($\alpha = 78^\circ$) than that of *i*- 3^+ ($\alpha = 87^\circ$). Although the pyrimidine plane and the adjacent C–N double bond were almost coplanar, the phenylene linker between the two imine moieties is distorted with a Cu–N(imine)–C(1-phenylene)–C(2-phenylene) dihedral angle of 27° (Figure S3). This distortion probably originates from the avoidance of atomic contacts between the bulky anthryl groups.

^1H NMR spectra of $2 \cdot (\text{BF}_4)_2$ in CD_2Cl_2 displayed four methyl signals. Consideration of shielding effects and integrated values suggests that one ($\delta = 2.38$ ppm) is attributed to an *oo*-isomer, another one ($\delta = 1.82$ ppm) to an *ii*-isomer, and the remaining two ($\delta = 2.39$ ppm, 1.75 ppm) to an *io*-isomer (Figure 2b). The peak shifts and integrated values of the other signals and the ^1H - ^1H COSY spectrum were well assigned and agreed with the interpretation of the methyl signals (Figure S4). The three isomers coexisted with an *oo*-*io*-*ii*-ratio of 49%:42%:9% at room temperature. This ratio corresponds to the statistic distribution of *o*:*i* = 7:3, considering that *io*- is doubled by *io*- and *oi*- configuration ($49\%:42\%:9\% = (0.7 \times 0.7):(2 \times 0.7 \times 0.3):(0.3 \times 0.3)$). The *i/o* ratio of $2 \cdot (\text{BF}_4)_2$ (*i/o* = 0.4) is smaller than that of $1 \cdot \text{BF}_4$ (*i/o* = 1.1), suggesting that the copper center is sterically more crowded in $2 \cdot (\text{BF}_4)_2$ than in $1 \cdot \text{BF}_4$.

The CV of $2 \cdot (\text{BF}_4)_2$ recorded at 293 K shows two redox waves at $E^\circ = 0.61$ and 0.74 V vs. Ag^+/Ag (Figure 3c). The redox couple at a more positive potential is assignable to the copper centers with an *i*-oriented methylpyrimidine ring of the *ii*- and *io*-isomers. Another redox wave is assigned to the copper centers with an *o*-oriented methylpyrimidine ring of the *oo*- and *io*-isomers. No additional redox waves were detected in the CV, confirming the absence of a mixed-valence state in 2^{3+} (i.e., the one-electron-oxidized form of 2^{2+}). The absence is possibly explained by the twisting of the phenylene linker in the L2 ligand, as mentioned above in the section concerning crystallography. The twist causes weak or almost no conjugation on the two imine bonds, yielding negligible electronic communication between the two copper ions. The slight positive shift of the redox potential from $1 \cdot \text{BF}_4$ ($E^\circ = 0.56$ and 0.71 V) to $2 \cdot (\text{BF}_4)_2$ ($E^\circ = 0.61$ and 0.74 V) can also be attributed to the congested structure, which prevents the formation of a favorable structure of Cu^{II} .

The CV waves of $2 \cdot (\text{BF}_4)_2$ appear broader than those of $1 \cdot \text{BF}_4$ (Figure 3c). The broader waves and larger separation between the oxidation and reduction peaks were likely due to the slower electron-transfer rate in $2 \cdot (\text{BF}_4)_2$ than in $1 \cdot \text{BF}_4$. The slower electron transfer might be attributable to the congested structure around each copper atom, which would interfere structurally with each other, thereby disturbing the structural rearrangement for the redox process. The CVs of $2 \cdot (\text{BF}_4)_2$ recorded at 243 K show further broadening of the redox peaks owing to the slower electron-transfer rate at low temperatures (Figure 3d).

In conclusion, we synthesized mono- and dinuclear 4-methyl-2-pyrimidinylimine complexes $1 \cdot \text{BF}_4$ and $2 \cdot (\text{BF}_4)_2$, respectively. $1 \cdot \text{BF}_4$ formed two isomers, and $2 \cdot (\text{BF}_4)_2$ formed

three, as expected from the single or double inversion of the pyrimidine rings. CVs show that the negative redox potential shifts from *i*- to *o*- through pyrimidine inversion also works in these structures. The inversion in $1 \cdot \text{BF}_4$ was supported by crystal structure analysis, which allowed the selective isolation of both *i*- and *o*-isomers in the crystalline state. Independent rotation at each unit explained the behavior of $2 \cdot (\text{BF}_4)_2$. The different inversion and redox behaviors of $3 \cdot \text{BF}_4$, $1 \cdot \text{BF}_4$, and $2 \cdot (\text{BF}_4)_2$ were explained by intramolecular steric effects. The behavior of $2 \cdot (\text{BF}_4)_2$ was particularly affected by the steric interference between its two monomer units. These results provide new insights into the assembly of redox-active molecular machinery units within short distances.

The authors acknowledge Grants-in-Aid from MEXT of Japan (Nos. 20750044, 20245013, and 21108002; area 2107 (Coordination Programming)), the Global COE Program for Chemistry Innovation.

References and Notes

- † Present address: Department of Materials and Life Science, Seikei University, 3-3-1 Kichijoji-kitamachi, Musashino, Tokyo 180-8633
- †† Present address: Department of Chemistry, Graduate School of Science, Hiroshima University, 1-3-1 Kagamiyama, Higashi-Hiroshima, Hiroshima 739-8526
- 1 J. E. Green, J. W. Choi, A. Boukai, Y. Bunimovich, E. Johnston-Halperin, E. Delonno, Y. Luo, B. A. Sheriff, K. Xu, Y. S. Shin, H.-R. Tseng, J. F. Stoddart, J. R. Heath, *Nature* **2007**, *445*, 414.
- 2 a) Y. Tanaka, A. Inagaki, M. Akita, *Chem. Commun.* **2007**, 1169. b) S. Venkataramani, U. Jana, M. Dommaschk, F. D. Sönnichsen, F. Tuczek, R. Herges, *Science* **2011**, *331*, 445.
- 3 a) N. Koumura, R. W. J. Zijlstra, R. A. van Delden, N. Harada, B. L. Feringa, *Nature* **1999**, *401*, 152. b) M. von Delius, E. M. Geertsema, D. A. Leigh, D.-T. D. Tang, *J. Am. Chem. Soc.* **2010**, *132*, 16134.
- 4 a) A. Livoreil, J.-P. Sauvage, N. Armaroli, V. Balzani, L. Flamigni, B. Ventura, *J. Am. Chem. Soc.* **1997**, *119*, 12114. b) M. C. Jiménez, C. Dietrich-Buchecker, J.-P. Sauvage, *Angew. Chem., Int. Ed.* **2000**, *39*, 3284.
- 5 K. Nomoto, S. Kume, H. Nishihara, *J. Am. Chem. Soc.* **2009**, *131*, 3830.
- 6 H. Nishihara, *Chem. Lett.* **2014**, *43*, 388.
- 7 M. Nishikawa, S. Kume, H. Nishihara, *Phys. Chem. Chem. Phys.* **2013**, *15*, 10549.
- 8 Crystallographic data reported in this manuscript have been deposited with Cambridge Crystallographic Data Centre as supplementary publication no. CCDC-988627, 988628, and 988629. Copies of the data can be obtained free of charge via <http://www.ccdc.cam.ac.uk/conts/retrieving.html> (or from the Cambridge Crystallographic Data Centre, 12, Union Road, Cambridge, CB2 1EZ, UK; fax: +44 1223 336033; or deposit@ccdc.cam.ac.uk).
- 9 C. L. Merrill, L. J. Wilson, T. J. Thamann, T. M. Loehr, N. S. Ferris, W. H. Woodruff, *J. Chem. Soc., Dalton Trans.* **1984**, 2207.
- 10 M. Schmittel, C. Michel, S.-X. Liu, D. Schildbach, D. Fenske, *Eur. J. Inorg. Chem.* **2001**, 1155.
- 11 Supporting Information is available electronically on J-STAGE.
- 12 a) M. Ruthkosky, C. A. Kelly, F. N. Castellano, G. J. Meyer, *Coord. Chem. Rev.* **1998**, *171*, 309. b) M. Ruthkosky, F. N. Castellano, G. J. Meyer, *Inorg. Chem.* **1996**, *35*, 6406.
- 13 In the structural analysis, remaining electron density in the void was accounted using the SQUEEZE routine in PLATON. P. van der Sluis, A. L. Spek, *Acta Crystallogr., Sect. A: Found. Crystallogr.* **1990**, *46*, 194.